# RECURSIVE MODELING OF A MAGNETO-RHEOLOGICAL DAMPER

*S. Kaul*

Department of Mechanical and Aeronautical Engineering
University of Pretoria, Pretoria, South Africa, 0002
Email: sudhir.kaul@up.ac.za

**ABSTRACT**

This paper proposes the use of three recursive system identification techniques for modeling a magneto-rheological (MR) damper. The results of the three models are compared to one another and to two parametric models that have been commonly used in the literature for modeling these dampers. An experimental set-up using an MR damper, that is fabricated in-house, is built and used for data collection. The collected data is used for system identification at varying input conditions and the results from the system identification models are compared to the measured data as well as to the parametric models. It is seen that while the parametric models work well within limited bounds of input variables, these models cannot be used outside the range of these bounds since any significant change in the inputs or operating conditions requires a new characterization of the model parameters. The recursive system identification models, instead, continuously update the model parameters as and when data becomes available, as demonstrated by the three models presented in this paper. The determination of the regressor can present a significant challenge in the implementation of recursive models; this paper uses an iterative method coupled with statistical measures in order to establish the regressor that is then used for all three system identification models. The advantages of the recursive models are conclusively established by a lower root mean square error (RMSE) and a better representation of the hysteretic and saturation phenomena exhibited by the MR damper, in addition to an improved model tracking. This provides an inherent advantage over the parametric models, thereby making the recursive models specifically conducive to adaptive control algorithms.

*Keywords:* Magneto-rheological, Recursive Least Square, System Identification

## 1. INTRODUCTION

Magneto-rheological (MR) fluids are suspensions of micron-size, magnetizable particles dispersed in an organic or an aqueous carrier fluid. The fluid behaves like a viscous liquid in the absence of a magnetic field. However, the introduction of an external magnetic field instantly increases the yield strength of the fluid resulting in a semi-solid, visco-plastic behavior of the fluid. This transition is completely reversible and can be achieved in milli-seconds (Carlson, 2005; Goncalves et al., 2006). This property of MR fluids has been used by researchers to provide a variable damping force resulting from an MR fluid actuator or an MR fluid damper. While there have been other smart materials like ferroelectric fluids, piezoelectric elements, shape memory alloys, etc. that have been successfully used for structural control, MR fluids exhibit a unique combination of completely reversible effect, very low response time, high durability and very low energy requirements that make them suitable for structural control in a wide variety of applications. Additionally, an MR fluid control device is semi-active, and as such does not have the potential to destabilize the overall system.

The last two decades have seen a phenomenal increase in the usage of MR fluids. A list of many commercial products that have successfully used MR fluids is available (Carlson, 2005). This paper provided some guidelines to estimate the size of an MR device using empirical equations. The two modes of most common usage of MR fluid devices are direct shear mode and valve mode (Olabi and Grunwald, 2007). A third mode of usage, called the squeeze mode, was also listed and briefly discussed by the authors. Vibration control is the most widely researched application of MR fluids. Usage of MR devices has been experimentally demonstrated for seismic control (Yi et al., 2001). Two semi-active control algorithms were used to implement control at several excitation levels. The performance of the MR damper was concluded to be superior to other comparable systems. An MR foam damper has been used to isolate a single degree-of-freedom system from harmonic and random excitation (Sarigul-Klijn et al., 2007). Positive control characteristics were exhibited by the MR device under several experimental conditions. A quarter-car model has been used to demonstrate the benefits of using an MR damper for suspension control (Rashid et al.,

2007). It was shown that ride comfort and handling characteristics could be simultaneously improved by using semi-active control algorithms. MR fluid has been used to build a mixed mode isolator, called the MR mount (Hong and Choi, 2005), in order to isolate a base structure from an externally excited lumped mass. A Bingham plastic model was also developed to estimate the damping force of the mixed mode mount. The use of MR fluid was incorporated into the design of a conventional fluid mount in order to control the opening or closing of the inertia track in the fluid mount (Ahn et al., 1999). The isolation performance of the fluid mount was seen to improve.

The intrinsically non-linear and highly hysteretic behavior of MR dampers has been studied by researchers and numerous models have been proposed in existing literature. The proposed models range from parametric models with idealized mechanical elements used to represent different aspects of the behavior of MR dampers to significantly complex non-parametric models. A comprehensive model of an MR damper has been presented by researchers to accurately predict the damping force over a wide range of operating conditions (Spencer et al., 1997). This model is essentially parametric, and is based on the Bouc-Wen hysteresis model. The MR damper was characterized by using a least squares algorithm to compute all the necessary system parameters by the authors. This characterization was governed by the time varying Bouc-Wen parameter which is in turn governed by a stiff non-linear differential equation. Alternate forms of this model have been used by other researchers with varying degrees of success (Savaresi et al., 2005). A high order mathematical function has also been investigated to capture the relationship between input current and the resulting damping force (Simon, 2001). A Bingham plastic model has been used to compute the damping constant and the yield force of the MR damper as a function of input current (Hong and Choi, 2005). Neural networks based models have also been used by some researchers to model the characteristics of the MR damper (Xia, 2003). A neural network based inverse model was developed in this work in order to predict the voltage input required for producing a damping force from an MR damper. The inherent disadvantage of Neural Networks models is the black-box nature of the models. A polynomial model between input velocity and the corresponding damping force has been investigated by researchers (Du et al., 2005). An eleventh order polynomial function was selected after a trial and error process. Algorithms based on wavelets and ridgelets analysis have been proposed in order to model the characteristics of an MR damper (Jin et al., 2005). A neural network based recursive method has been used for modeling MR dampers (Boada et al., 2009). The modeling technique used by the authors is based on the recursive least squares method. Results

obtained in this work were comparable to a Bouc-Wen parametric model and the authors discussed the advantages of recursive models over parametric models with regards to computational time.

Most of the models proposed in existing literature for modeling the behavior of MR dampers are primarily parametric, attempting to capture properties of the damper with the incorporation of mechanical elements. There are some non-parametric models in existing literature but most of these models are very complex. This paper meticulously determines a regressor vector to capture the characteristics of the MR damper and presents three recursive system identification models with time-varying parameters that can be integrated with an adaptive control algorithm in order to implement structural control with an MR damper for applications with varying system dynamics. The proposed models will be especially beneficial for MR dampers over large ranges of voltage or current inputs, input displacement amplitudes and excitation frequencies, without requiring any re-configuration of the basic model or any new computation of the system parameters.

The next section, Section 2, briefly outlines the three system identification models and two parametric models that have been commonly used in the existing literature. Section 3 describes the experimental set-up that is used for data collection and model validation. The results are discussed in Section 4, comparing the results of the system identification models with one another and with the results of the parametric models. Section 5 draws overall conclusions and outlines possible future work.

## 2. MODELING

This section presents three recursive system identification techniques used for modeling the MR damper in this paper. Two parametric models that have been commonly used in the literature for modeling MR dampers are also discussed in this section and the modeling results are compared to the results of the recursive models.

### 2.1 Recursive Identification Models

The solution to a general system identification problem with a single output can be mathematically expressed as follows:

$$\hat{y}_k = \phi_k^T \hat{\theta} \qquad (1)$$

In Eq. (1), $\hat{\theta}$ is the $n \times 1$ column matrix consisting of estimated parameters, $\hat{y}_k$ is the estimated output and $\phi_k^T$ is the $1 \times n$ vector, also called the regressor vector, assumed to be known for the specific system being identified. If multiple data points are available for the

measured output, $\overline{y}_1$, $\overline{y}_2$, ..., a least squares solution to determine $\hat{\theta}$ can be expressed as:

$$\hat{\theta} = \left(\Phi^T \Phi\right)^{-1} \Phi^T Y \qquad (2)$$

In Eq. (2), $Y$ is the $t$ x $1$ column matrix consisting of $t$ measured values of the output and $\Phi$ is the $t$ x $n$ matrix consisting of regressor vectors $\phi_1^T$, $\phi_2^T$, ... as its rows. Since all the measured values are used together in Eq. (2), the estimation is generally called the Batch Least Squares (BLS) estimate. The existence of $\left(\Phi^T \Phi\right)^{-1}$ is a necessary condition for the BLS estimation process (Astrom and Wittenmark, 1995; Ljung and Soderstrom, 1985), and is called the excitation condition in system identification literature. Lack of excitation can result in the parameter estimates being highly sensitive to noise. This problem has been overcome in this work by using a higher order input and the results are further validated by computing the variance of estimated parameters. It may be noted that this paper uses BLS only to establish starting guesses for the recursive identification process, as outlined in the remaining part of this section.

Since the model order for the MR damper is not well understood, the regressor vector needs to be assessed before any system identification can be carried out. This is done in this paper by adding parameters to the regressor iteratively till the mean square error (MSE), the residual error and the loss function do not reduce appreciably any more. Additionally, the Fischer statistic is used in order to eliminate any subjectivity in deciding the model order of the regressor. A Fischer statistic of less than 10 (Astrom and Wittenmark, 1995; Montgomery et al., 2008) is deemed to be statistically insufficient to support an increase in the model order.

Since the characteristics of an MR damper are inherently non-linear, showing significant changes in the force-velocity relationship with changing displacement amplitudes, excitation frequencies and voltage inputs, a recursive system identification technique should be more appropriate for successful modeling of the damper. The iterative formulation of the Least Squares technique, called as the Recursive Least Squares (RLS), estimates the parameters as follows:

$$\hat{\theta}(t) = \hat{\theta}(t-1) + K(t)\left[\overline{y}(t) - \phi^T(t)\hat{\theta}(t-1)\right] \qquad (3)$$

In Eq. (3), $\overline{y}(t)$ is the measured system response at time interval $t$, with $\hat{\theta}(t-1)$ and $\hat{\theta}(t)$ being the time-varying parameter estimates at time intervals $t$-$1$ and $t$ respectively. $K(t)$ is the connecting variable between the estimation parameter and $P(t)$ and is computed as:

$$K(t) = P(t-1)\phi(t)\left[\lambda + \phi^T(t)P(t-1)\phi(t)\right]^{-1} \qquad (4)$$

In Eq. (4), $0 < \lambda \leq 1$ is the forgetting factor used to mitigate the influence of errors from previous measurements in order to minimize their influence on current estimates. The choice of a forgetting factor is based on particular aspects of system dynamics, with the selection of a low factor generally adopted for tracking rapid parameter variations (Ljung and Soderstrom, 1985). It may be noted that the inverse in Eq. (4) is the inverse of a scalar for a single output system. A large positive definite matrix is generally used as the starting value of $P$, $P(0)$. The time-varying matrix $P$ is computed as follows:

$$P(t) = \left[I - K(t)\phi^T(t)\right]\frac{P(t-1)}{\lambda} \qquad (5)$$

In Eq. (5), $I$ is an identity matrix, the order of $I$ is equal to the order of $P$. A starting value of $\hat{\theta}(0)$ is required in order to iteratively estimate the parameters using Eqs. (3), (4) and (5), where $\hat{\theta}(0)$ may be arbitrarily selected. In this paper, the starting guess is based on an initial run using a BLS estimation from the first few points of the collected data.

Least Mean Square (LMS) algorithm is widely used in Neural Networks and results in a uniform zone of uncertainty for all the estimated parameters. However, the resulting convergence of parameters is non-uniform, in contrast to the RLS algorithm. This paper uses LMS as an alternate to the RLS algorithm since the composition of the regressor for an MR damper is not well understood, thereby questioning the validity of the use of RLS when the regressor does not satisfy the necessary conditions. The LMS parameter estimation uses an alternate form of the forgetting factor and is expressed as follows:

$$\hat{\theta}(t) = \hat{\theta}(t-1) + \gamma_1 \phi(t)\left[\overline{y}(t) - \phi^T(t)\hat{\theta}(t-1)\right] \qquad (6)$$

In Eq. (6), the use of $\gamma_1$ is analogous to the use of the forgetting factor, $\lambda$, in RLS. An approximate equivalence can be established between the two factors as $\gamma_1 \approx 1 - \lambda$, with $0 < \gamma_1 \leq 1$ (Astrom and Wittenmark, 1995).

The Projection algorithm is the third recursive parameter identification algorithm used in this paper for identification of an MR damper. The parameter estimation of the Projection algorithm is expressed as:

$$\hat{\theta}(t) = \hat{\theta}(t-1)$$
$$+ \frac{\gamma_2 \phi(t)}{\overline{\alpha} + \phi^T(t)\phi(t)}\left[\overline{y}(t) - \phi^T(t)\hat{\theta}(t-1)\right] \qquad (7)$$

All the variables in Eq. (7) are identical to the earlier defined variables, $\overline{\alpha}$ is an additional constant in Eq. (7) and is selected to be strictly greater than zero in order to

avoid division by zero. A value of 0.1 has been used for $\bar{\alpha}$ in this paper. The other constant in Eq. (7) must be chosen such that $0 < \gamma_2 < 2$. The distinct advantage of the Projection algorithm is its simplicity and the reduced computational expense, although the algorithm may result in slower convergence. It may be noted that the identification results can vary with different choices of the forgetting factors, thereby making it difficult to compare results between different identification methods. This work has attempted to use analogous forgetting factors between the recursive identification methods in order to mitigate difficulties in comparing the results.

In order to establish model order and identify the regressor, BLS is used iteratively. The model order and regressor coefficients are changed over iterations, with the addition of one regression coefficient per iteration. MSE and the Fischer statistic are compared between the two models till there is no significant reduction in MSE. The variance of the estimated parameters is also computed in order to assess the sensitivity of the parameters to noise as well as excitation. The model identification relationship for the MR damper can be defined as:

$$\hat{f}(t) = \phi^T(t-1)\hat{\theta} \qquad (8)$$

In Eq.(8), $\hat{f}(t)$ is the estimated damping force and $\phi^T(t-1)$ is the regressor vector. The composition of the regressor vector is selected so as to consist of the history of previous damping forces, displacement amplitudes, velocity inputs and a combination of these variables. The regressor vector established for the damper used for experimentation in this paper is as follows:

$$\phi^T(t-1) = \begin{bmatrix} x(t-1),\ x(t-2),\ x(t-3), \\ \dot{x}(t-1),\ |\dot{x}(t-1)|f(t-1), \\ f(t-1), f(t-2),\ f(t-3) \end{bmatrix} \qquad (9)$$

The regressor in Eq. (9) is *1 x 8* consisting of three displacement coefficients, three force coefficients, one velocity coefficient and one combined coefficient (between velocity and force). Since the model order has been established iteratively, further tests are run at different voltage levels in order to confirm that the errors (or residuals) remain Normally distributed and that the errors don't exhibit auto-correlation. One such example can be seen in Fig. 1 which shows the Normal probability plot of the residuals. As can be seen in Fig. 1, the errors generally lie along the straight line, thereby satisfying the Normal distribution requirement of the residuals. The Durbin-Watson test is run at two voltage levels to detect the presence of auto-correlation, both tests confirm the validity of the null hypothesis (Montgomery et al., 2008), implying that there is no auto-correlation in the residuals. This establishes the validity of the regressor in Eq. (9),

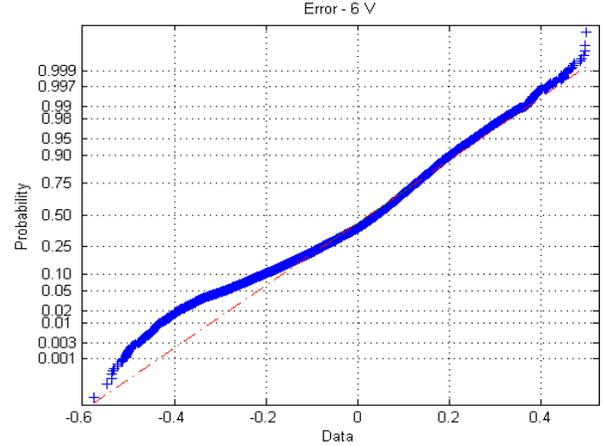which will be used for all three recursive models in the subsequent section.



Figure 1 Normal Probability Plot - Residuals

## 2.2 Parametric Models

Parametric models have been frequently used for modeling MR dampers in existing literature. The most commonly used parametric model in the MR modeling literature is the modified Bouc-Wen model (Spencer et al., 1997). The tangent hyperbolic model and the Bingham plastic model have also been used by some researchers (Hong and Choi, 2005; Simon, 2001). The results of the three system identification models that are presented in the previous sub-section will be compared with two of the above listed parametric models.

The most basic form of the Bouc-Wen model consists of stiffness and damping constants in addition to a time-varying parameter and is expressed as follows:

$$F = kx + c\dot{x} + \alpha z \qquad (10)$$

In Eq. (10), $k$ is the stiffness constant, $c$ is the damping constant, $z$ is the time varying parameter, $\alpha$ is a constant and $F$ is the damping force, with $x$ and $\dot{x}$ being the displacement and velocity amplitudes. The time varying parameter is governed by another first order differential equation, expressed as:

$$\dot{z} = -\gamma|\dot{x}| z |z|^{n-1} - \beta\dot{x}|z|^n + A\dot{x} \qquad (11)$$

In Eq. (11), $\beta$, $\gamma$, $n$ and $A$ are the additional constants required to compute the time history of $z$. It may be noted that several modified forms of the Bouc-Wen model have been used in existing literature (Savaresi et al., 2005; Spencer et al., 1997) in order to capture specific aspects of the MR damper being modeled. However, the identification of the parameters for the model in Eqs. (10) and (11) may result in non-unique constants and an over-parameterized model.

34

The tangent hyperbolic model consists of the applied current and the relative velocity as the input variables to determine the resulting force of the MR damper. The damping force is expressed as follows (Simon, 2001):

$$F = (\alpha_1 I + \alpha_2)\left[Tanh(\alpha_3 \dot{x}) + \alpha_4 \dot{x} + \alpha_5\right] \quad (12)$$

In Eq. (12), $\dot{x}$ is the relative velocity input to the MR damper, $I$ is the applied current and $\alpha_1$, $\alpha_2$, $\alpha_3$, $\alpha_4$, and $\alpha_5$ are empirical constants determined by using a best-fit technique.

The Bingham plastic flow model of the MR damper is another model that has been commonly used in the literature but will not be discussed in this paper. It is another parametric model consisting of coefficients relating the damping force to relative velocity and input current (Du et al., 2005; Hong and Choi, 2005).

## 3. EXPERIMENT

This section discusses the experimental set-up that is used in this work for data collection. The data is used for building alternate models and data collection is subsequently repeated for model validation. The MR damper that has been used for data collection was made in-house; a similar set-up has been used by other researchers for experimentation (Olabi and Grunwald, 2007; Yi et al., 2001) means of a pressure adhesive on both sides of the foam. The overall construction of the MR damper is shown in Fig. 2.
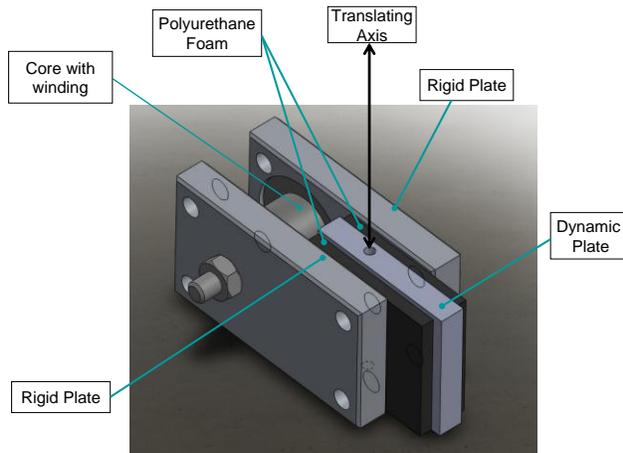


Figure 2 Foam-based MR Damper

The MR damper consists of two layers of open-cell polyurethane foam, saturated with MR fluid. Each layer of the foam is approximately 3 mm thick without any pre-compression. Open-cell polyurethane foam contains voids that allow a higher absorption of the MR fluid and is generally preferable to closed-cell foam. The fluid used for the experiment, MR-140 CG, was procured from LORD Corporation. Each layer of the saturated foam is attached to a rigid plate on one side and the common dynamic plate on the other. The dynamic plate is sandwiched between the two layers of foam, as shown in Fig. 2. The two rigid plates, one on each side, and the dynamic plate at the center are dimensioned such that each layer of foam is retained under a slight pre-compression after the system is assembled together. The layers of the foam are attached to the plates. The MR damper is used in shear mode with the dynamic plate connected to a load cell through an actuator rod on one side, and to a controlled displacement input from a hydraulic actuator on the other side. An electromagnetic circuit required to control the MR actuator is placed adjacent to the foam and consists of a mild steel core with an insulated copper wire winding. The electromagnet used for this experiment consists of 400 windings of 0.224 mm diameter wire with a coil resistance of approximately 10 Ω. The voltage input to the electromagnet is varied between 0V and 10V. The current draw corresponding to the voltage input is measured as well. The damping force resulting from the MR damper is measured by means of a load cell. The inputs to the MR damper consist of sinusoidal displacement amplitudes ranging from ± 0.25 mm to ± 1 mm at varying frequencies, ranging from 2 Hz to 18 Hz. The reaction load is measured by the load cell at a sampling frequency of 500 Hz. The reaction load and the input displacement are collected by an eDAQ data acquisition system and the corresponding velocity is computed by using numerical differentiation that is implemented with the use of the central difference algorithm.
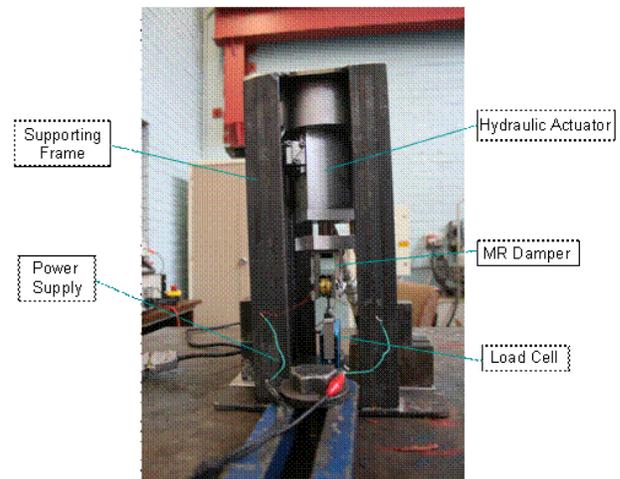


Figure 3 Experimental Set-up

The overall test set-up with all the instrumentation is shown in Fig. 3. Fig. 4 shows the force-velocity curves from the measured data with sinusoidal displacement

amplitude of 0.25 mm at an input frequency of 12 Hz, as the voltage is increased from 0V to 10V. The MR damper acts as a simple viscous damper when there is no voltage supply input to the system, as can be seen from the force-velocity plot in Fig. 4 at 0V. As the voltage increases, the MR damper exhibits higher damping before reaching a threshold, called saturation. The saturation property of the MR damper can also be observed in Fig. 4 at higher velocity levels, with the increase in voltage.
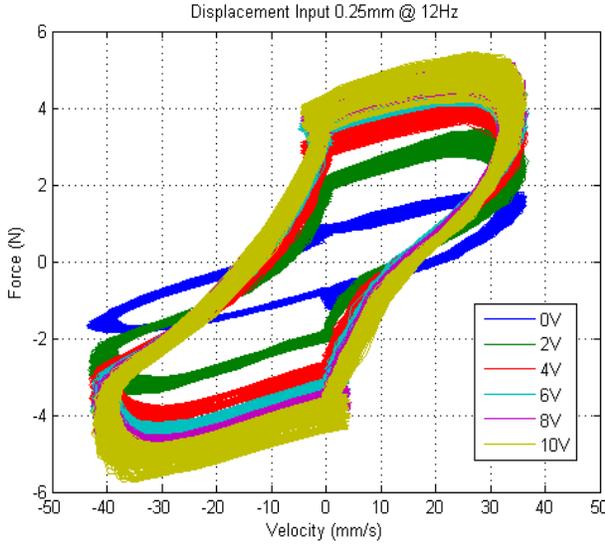


Figure 4 Measured Force-velocity Data at ± 0.25 mm @ 12 Hz

## 4. RESULTS

This section presents the results of system identification using the experimental data collected from the MR damper, as discussed in the previous section. The two parametric models, discussed in Section 2, are also characterized and compared to the system identification models.

Table 1 lists the results for the BLS model using the regressor defined in Eq. (9). Separate characterization is performed for each voltage level. In Fig. 5, the resulting BLS model is compared to the measured data at 6V. The root mean square error (RMSE) is used all through the paper to compare the measured data with the predicted outcome from the models. It may be noted that the RMSE is the lowest for the BLS model at 0V and keeps increasing with higher voltage levels, as can be seen in Table 1. Although a BLS model can be characterized to fit the data from all voltage levels together, such a model results in a significantly higher RMSE and yields poor model tracking. This can be attributed to the increasingly hysteretic behavior of the MR damper with increasing voltage as well as to the more pronounced saturation at higher voltage levels. These shortcomings can be overcome by adopting the recursive models. Additionally, the recursive models will eliminate the need for separate characterization at different voltage levels, which is a shortcoming of the parametric models as well.

In order to demonstrate the application of the recursive system identification techniques, a new test is run with the same experimental set-up as explained in the previous section. However, the voltage input to the MR damper is continuously varied, increasing from 0V to 10V, so as to simulate the working of the damper through the entire range of the damping force. Fig. 6 shows a comparison of the predicted output of the RLS model to the measured data (i.e. f versus $\hat{f}$). As can be seen, the estimated response closely tracks the measured response except for a few outliers. The outliers coincide with the instances of changes in input voltage, when the RLS algorithm results in a change of estimated parameters.

Table 1 Computed BLS Parameters

| | | $\theta_1$ | $\theta_2$ | $\theta_3$ | $\theta_4$ | $\theta_5$ | $\theta_6$ | $\theta_7$ | $\theta_8$ | RMS Error |
|---|---|---|---|---|---|---|---|---|---|---|
| | | | | | | BLS Parameters | | | | |
| Input Voltage | 0 V | -11.2864 | 12.6534 | -0.8839 | 0.0347 | 0.0016 | 1.3257 | -1.0567 | 0.583 | 0.0549 |
| | 2 V | -26.3067 | 41.3079 | -13.5689 | 0.0582 | -0.0032 | 1.6363 | -1.3589 | 0.5213 | 0.1266 |
| | 4 V | -32.4148 | 55.3988 | -19.3003 | 0.0874 | -0.0065 | 1.5679 | -1.3667 | 0.5024 | 0.1596 |
| | 6 V | -25.0104 | 47.4192 | -17.4776 | 0.0945 | -0.0085 | 1.537 | -1.4452 | 0.5824 | 0.1641 |
| | 8 V | -23.3117 | 46.7416 | -17.4751 | 0.1005 | -0.0087 | 1.4923 | -1.4346 | 0.5855 | 0.169 |
| | 10 V | -26.801 | 51.9174 | -18.8339 | 0.1042 | -0.0077 | 1.4753 | -1.3861 | 0.5473 | 0.1757 |

An example of the varying parameter history is shown in Fig. 7 for one of the eight parameters. It may be noted that the parameter fluctuation corresponds to the changing input voltage till a certain threshold. The parameter stabilizes for higher voltage levels because the rate of change of the damping force reduces at these higher voltage levels, as can be seen from the measured data, shown in Fig. 4.
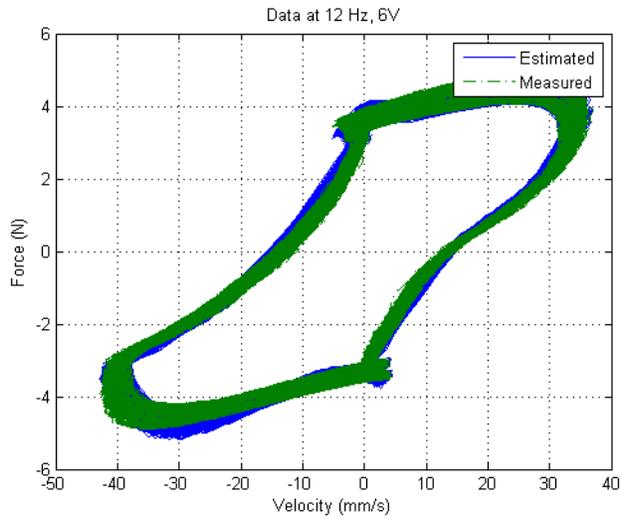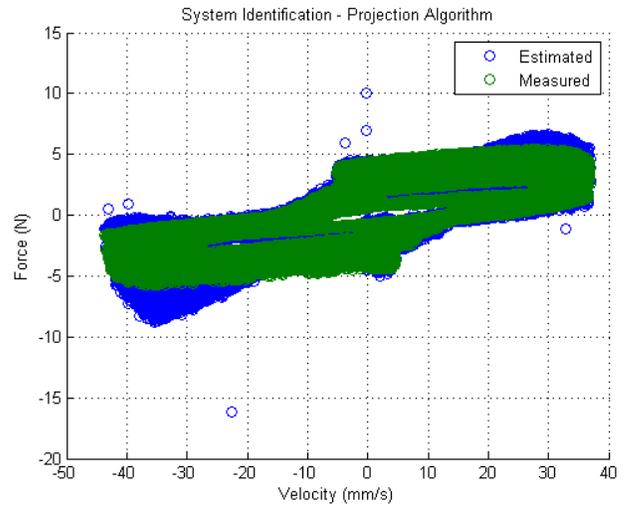
Figure 5 Force-velocity Curve – Comparison – 6V - BLS



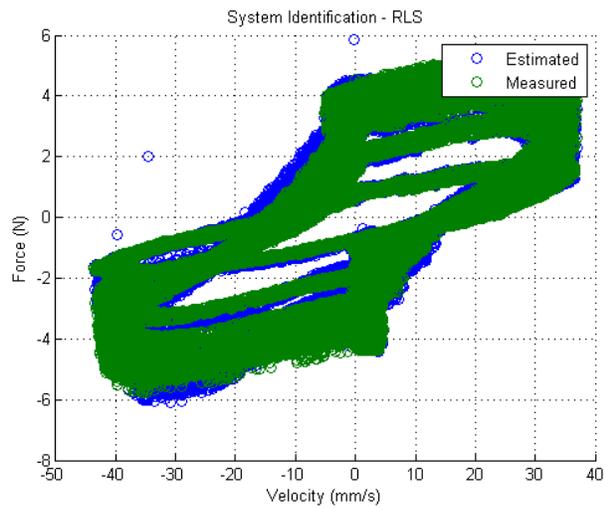Figure 8 System Identification Results – Projection Algorithm
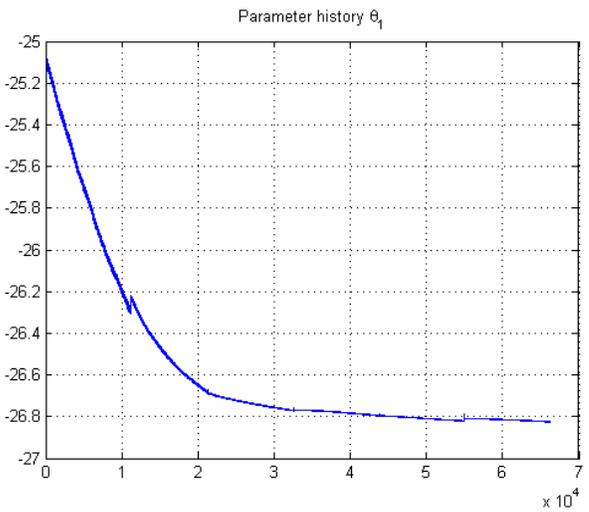


Figure 6 System Identification Results – RLS



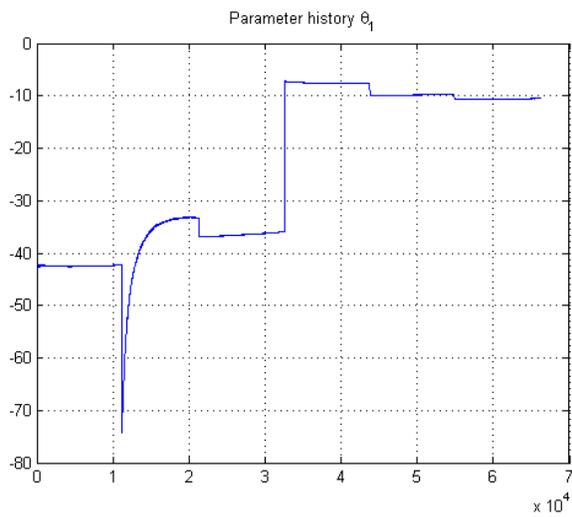Figure 9 Parameter History – $\theta_1$ – Projection Algorithm



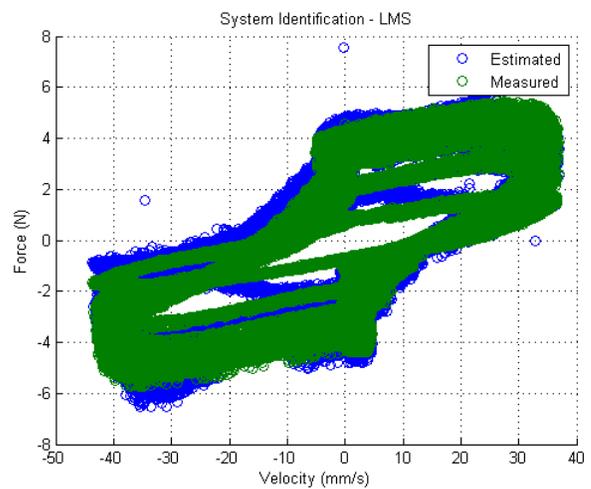Figure 7 Parameter History – $\theta_1$ – RLS



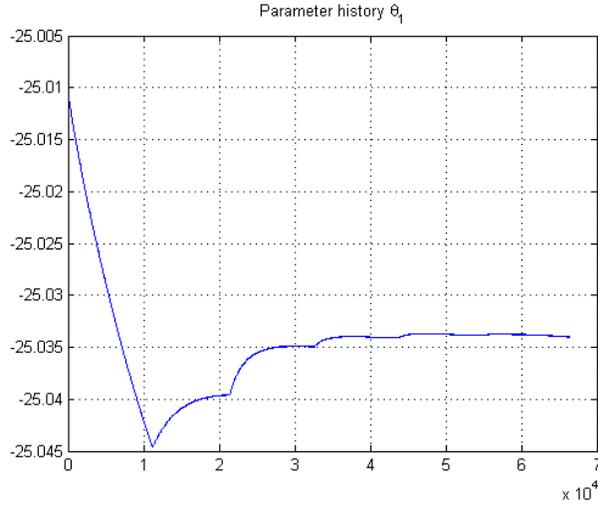Figure 10 System Identification Results – LMS
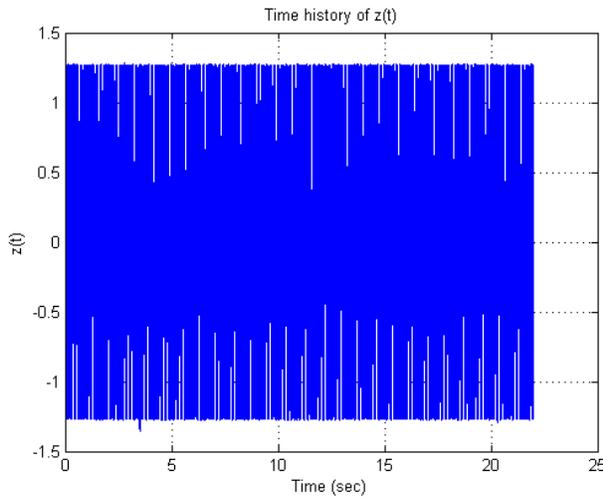
37

Figure 11 Parameter History – $\theta_1$ – LMS



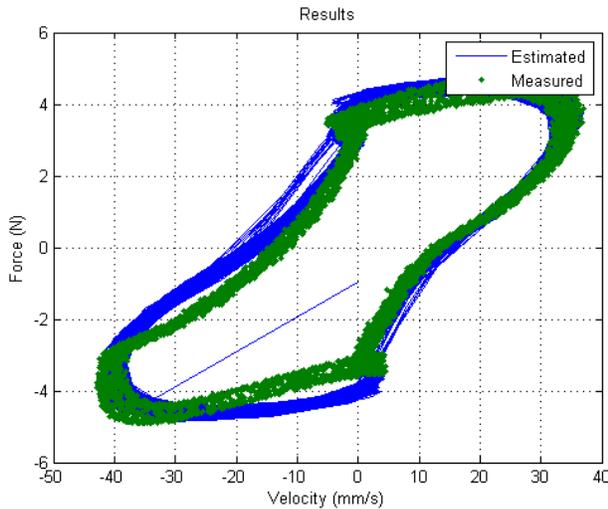Figure 12 Time history of z(t)



Figure 13 Bouc-Wen Parametric Model – 6V

This behavior of parameter variation is also exhibited by the other two recursive techniques used in this paper. The results from the other two recursive system identification techniques are shown in Figs. 8 and 10 with the corresponding parameter histories of $\theta_1$ shown in Figs. 9 and 11. It may be noted that the computational time for the three recursive techniques is pretty similar, ranging from 1.4% to 4% of each other.

The results from the Bouc-Wen based parametric model are shown in Figs. 12 and 13 for the input voltage of 6V and all the parameters for this model are listed in Table 2. The model parameters are determined by solving a least squares problem to minimize the difference between the measured force and the estimated force. The MATLAB® Optimization Toolbox function 'fmincon' (MATLAB User Guide, 2007) is used to solve the least squares problem and the stiff differential equation in Eq. (11) is solved by using 'ode15s' in MATLAB®. Fig. 12 shows the time history of, z(t), the time varying parameter of the Bouc-Wen model. The RMSE for the parametric model in Fig. 13 is comparable to the BLS and RLS models. However, the use of these model parameters for the same system with an input voltage of 10 V results in an increase in RMSE by 44%, necessitating re-computation of model parameters. Furthermore, the computational time required for the determination of the Bouc-Wen variables is orders of magnitude higher than the time required for characterizing the recursive models. The computed parameters corresponding to 10V input are listed in Table 2. Three of the seven parameters change significantly, ranging from 2.5% to 27%, as compared to the input voltage of 6V. This implies that any change in the inputs will have to correspond with a new characterization of the parametric model. This may not be feasible in a process with constantly changing input conditions.

Table 2 Computed Bouc-Wen Model Parameters

| | Stiffness Parameter (N/mm) | Damping Parameter (N-s/mm) | Bouc-Wen Parameters |
|---|---|---|---|
| Input Voltage: 6 V Displacement: ± 0.25 mm Frequency: 12 Hz | k = 11.8 | b = 0.03 | $\alpha$ = 1.183 $\beta$ = 12.2 $\gamma$ = 14.0 n = 2 A = 43.5 |
| Input Voltage: 10 V Displacement: ± 0.25 mm Frequency: 12 Hz | k = 13.6 | b = 0.038 | $\alpha$ = 1.15 $\beta$ = 12.15 $\gamma$ = 14.0 n = 2 A = 43.5 |

The results of another parametric model that is based on the usage of a higher order shape function are shown in Fig 14. This model uses the hyperbolic tangent function as expressed in Eq. (12). As can be assessed from Fig. 14,

the RMSE of this model is an order of magnitude higher than the Bouc-Wen parametric model and the model is not able to represent hysteretic characteristics. Additionally, the model parameters need to be re-computed for new input conditions. These constraints limit the usage of this model to very specific input conditions when the MR damper is used at very low frequencies.
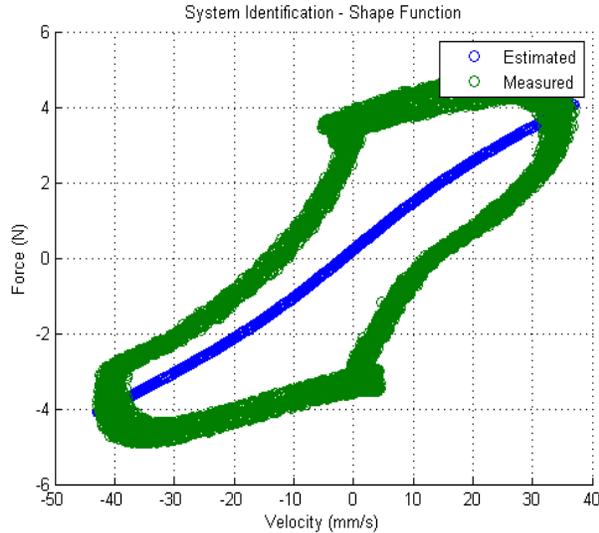


Figure 14 Shape Function Parametric Model – 6V

Out of the three recursive system identification techniques, RLS results in the lowest RMSE and is least sensitive to the choice of the algorithmic parameters. However, it may be noted that the use of RLS is based on assumptions about the behavior of the regressor and the residuals, which may not be valid all the time. Also, the use of RLS depends on the computation of two state variables, which can make it computationally more expensive for an on-line identification process, as compared to other recursive models. The RLS algorithm, therefore, cannot be the used as the default recursive identification method for all MR dampers and its usage should be evaluated on a case-by-case basis. LMS can be used as an alternative when the underlying assumptions for using RLS are not satisfied. Also, LMS requires the computation of only one state variable and results in a uniform variance, which could provide an advantage in certain on-line computations.

The advantages of recursive models over parametric models, like the ones suggested in (Spencer et al., 1997), have been discussed by other authors (Boada et al., 2009) as well. The determination of the variables associated with the parametric models can only be carried out by solving a non-linear optimization problem, which requires high computational effort and which may result in non-unique solutions.

## 5. CONCLUSIONS

This paper demonstrates the use of three recursive system identification techniques for modeling an MR damper, and compares the usage of these techniques to two commonly used parametric models. The recursive models establish a clear advantage over the parametric models, specifically when the MR damper is used over a wide range of input conditions. The use of the parametric models may not be viable in an on-line identification process since the sequential determination of the parameters can be computationally rigorous, especially for the Bou-Wen model. For the damper used in this study, the computation time for characterizing the Bouc-Wen model is seen to be orders of magnitude higher as compared to all three recursive models proposed in this paper. Additionally, the parametric models can result in non-unique constants and an over-parametrized model. However, the successful implementation of the recursive models is significantly dependant on the identification of the regressor vector. In this paper, a thorough procedure is followed in order to determine the regressor vector. The regressor is determined iteratively, using BLS and the Fischer statistic to assess the quality of fit of the models with changing regressors in order to minimize the possibility of under-fitting or over-fitting. Out of the three recursive models used in this paper, the RLS model proves to be superior and captures the two important properties of the MR damper, namely hysteresis and saturation, very well. The LMS model is a viable alternative to RLS without any associated penalty in terms of computational time for an on-line identification process. Furthermore, the LMS model can be used in those situations when the regressor is not completely known or when the underlying assumptions of the RLS model are not satisfied. The third recursive system identification technique based on Projection algorithm does not show any apparent advantages over the other two techniques discussed in this paper. The recursive models used in this paper are particularly suitable for adaptive control algorithms and will be used in future work for structural control using MR fluids.

### Acknowledgements

### REFERENCES

Ahn, Y.K., Ahmadian, M., Morishita, S., 1999. On the Design and Development of a Magneto-Rheological Mount, Vehicle System Dynamics, 32, 199-216.

Astrom, K.J., Wittenmark, B., 1995. Adaptive Control, 2nd Edition, Addison Wesley Longman, MA, USA.

Boada, M.J.L., Calvo, J.A., Boada, B.L., Diaz, V., 2009. Modeling of a Magnetorheological Damper by Recursive Lazy Learning. International Journal of Non-Linear Mechanics, doi:10.1016/j.ijnonlinmec.2008.11.019 (In Press).

Carlson, J.D., 2005. MR Fluids and Devices in the Real World. International Journal of Modern Physics B, 19 (7), 1463-1470.

Du, H., Sze, K., Lam, J., 2005. Semi-active H∞ control of Vehicle Suspension with Magneto-rheological Dampers, Journal of Sound and Vibration, 283, 981-996.

Goncalves, F.D., Koo, J., Ahmadian, M., 2006. A Review of the State of the Art in Magnetorheological Fluid Technologies – Part I: MR Fluid and MR Fluid Models, The Shock and Vibration Digest, 38 (3), 203-219.

Hong, S., Choi, S., 2005. Vibration Control of a Structural System Using Magneto-Rheological Fluid Mount, Journal of Intelligent Material Systems and Structures, 16, 931-936.

Jin, G., Sain, M.K., Spencer, B.F., 2005. Nonlinear Blackbox Modeling of MR-Dampers for Civil Structural Control, IEEE Transactions on Control Systems Technology, 13 (3), 345-355.

Ljung, L., Soderstrom, T., 1985. Theory and Practice of Recursive Identification, MIT Press, Cambridge, MA, USA.

MATLAB User Guide, 2007. Math Works, Natick, MA, USA.

Montgomery, D.C., Jennings, C.L., Kulahci, M., 2008. Introduction to Time Series Analysis and Forecasting, John Wiley & Sons, Hoboken, NJ, USA.

Olabi, A.G., Grunwald, A., 2007. Design and Application of Magneto-rheological Fluid, Materials and Design, 28, 2658-2664.

Rashid, M.M., Hussain, M.A., Rahim, N.A., Momoh, J.S., 2007. Development of a Semi-Active Car Suspension Control System Using Magneto-Rheological Damper Model, International Journal of Mechanical and Materials Engineering, 2 (2), 93-108.

Sarigul-Klijn, N., Lopez, I., Sarigul-Klijn, M., Karnopp, D., 2007. Vibration Mitigation Using Passive Active Tunable (PAT) System: Experimental Aspects, ASME Journal of Vibration and Acoustics, 129 (2), 209-216.

Savaresi, S.M., Bittanti, S., Montiglio, M., 2005. Identification of Semi-physical and Black-box Non-linear Models: The case of MR-dampers for Vehicles Control, Automatica, 41, 113-127.

Simon, D.E., 2001. An Investigation of the Effectiveness of Skyhook Suspensions for Controlling Roll Dynamics of Sport Utility Vehicles Using Magneto-Rheological Dampers, PhD Dissertation, Virginia Polytechnic Institute & State University, Blacksburg, VA, USA.

Spencer, B.F., Dyke, S.J., Sain, M.K., Carlson, J.D., 1997. Phenomenological Model of a Magneto-rheological Damper, ASCE Journal of Engineering Mechanics, 123 (3) 230-238.

Xia, P., 2003. An Inverse Model of MR Damper Using Optimal Neural Network and System Identification, Journal of Sound and Vibration, 266, 1009-1023.

Yi, F., Dyke, S.J., Caicedo, J.M., Carlson, J.D., 2001. Experimental Verification of Multi-Input Seismic Control Strategies for Smart Dampers, ASCE Journal of Engineering Mechanics, 127 (11), 1152-1164.